Laboratory Evaluation of Ethanol Corrosivity in Engine Oils for Gasoline Direct Injection (GDI) Flex-Fuel Engines

Charles Lima Bessa Assunção
PETROBRAS

Erika Christina Ashton Nunes Chrisman
Leila Yone Reznik
Federal University of Rio de Janeiro (UFRJ)

ABSTRACT

Modern engine oils must be aligned with the advancement of new engine technologies, designed to address various issues such as emission reduction, power enhancement, and fuel efficiency. In the context of the Brazilian market, the introduction of engines equipped with GDI flex fuel technology necessitates an evaluation of the impact of ethanol on the properties of the lubricating oil used, thereby providing a foundation for new developments. Formulations tailored to this market niche can be achieved through experimental design that concurrently and optimally encompasses components and operational conditions. Electrochemical impedance spectroscopy data have demonstrated potential in supporting the design of these new formulations, guiding the formulator in the appropriate selection of components. This technique, supplemented by other tests, indicated that ethanol contamination and the acidity generated from its incomplete combustion result in distinct effects on lubricating oils derived from GDI engines, particularly concerning corrosion in copper and iron materials. Despite greater contamination of the lubricating oil by fuel in engines powered by regular gasoline, there is a tendency for corrosive attack on copper components in engines powered by hydrated ethanol.

INTRODUCTION

Modern engine oils are composed of a varied base stocks and additives range, primarily for passenger vehicles in the automotive industry. These products must align with the development of new engine technologies designed to address issues such as emission reduction, power gain, and fuel economy [1].

In the Brazilian market, the introduction of flex-fuel engines with Gasoline Direct Injection (GDI) technology, starting in 2013 to meet then-program INOVAR-AUTO in Brazil, is an important area for evaluation. Until then, engine oils developed and were available in the market catered to the established Port Fuel Injection (PFI) flex-fuel engines, where fuel injection is performed via an intake manifold [2]. Unlike GDI engine, oil contamination, especially during engine start-up in low-temperature conditions, did not occur to the same extent. Due to the increasing use of ethanol as fuel, evaluating the effect of this alcohol on essential characteristics of engine oil, such as corrosion protection, is necessary for potential developments in the formulating industry [3].

Traditionally, the appropriate characteristics of engine oil formulations are achieved through trial-and-error procedures. Alternatively, using mathematical models provides an optimized product, speed in obtaining new formulations, cost efficiency, and greater operational safety. Conducting a significant number of experiments for mathematical modeling also allows for evaluating the influences of each component on the responses of interest and understanding the mechanisms of action of the substances in the final product [4].

Evaluating the influence of fuel on engine oil through engine tests is costly, given the use of adapted test benches with all necessary instrumentation for operational control, utilities, labor, and the engine's value. Therefore, studying procedures that reproduce real conditions and provide similarly modified samples compared to the original lubricant becomes relevant for a cheaper and expedited evaluation [5].

Typical analysis of engine oils, such as viscosity, oxidative stability, foam control, and corrosion protection, are used by formulators to control characteristics. Since these methodologies sometimes provide ambiguous and inconclusive results, developing new techniques is necessary. An example is the analysis of copper corrosivity by the ASTM D130 methodology, which presents a color scale for evaluating results with a high degree of subjectivity. In this context, electrochemical impedance spectroscopy, although still emerging in the evaluation of engine oils, provides sufficient data to assess the oil's corrosivity to different metals and alloys and allows for observing degradation characteristics of the lubricating mass and mechanisms of action of chemical additives on surfaces. The diagrams obtained by this technique, like Figure 1, combined with typical lubricant tests, lead to detailed conclusions about the entire system, providing

insights into formulations developments aligned with new engine technologies [6].

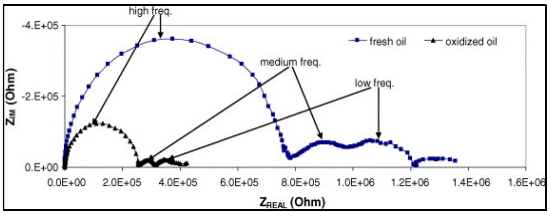

Figure 1. Impedance diagram of a typical industrial lubricant [7]

In this paper, an experimental design was used for the formulation of experimental engine oil, like SAE 0W 30 grade. With a known composition, this product was used in an artificial aging procedure, reproducing literature-available conditions for a GDI engine, including ethanol contamination. Real GDI engine tests were also conducted with commercial SAE 0W 30 engine oil, and the results obtained from feeding the equipment with hydrated ethanol were evaluated in comparison to artificial aging. All conclusions related to ethanol contamination for both engine oils were based on typical tests and electrochemical impedance spectroscopy, which proved to be a promising technique for evaluating engine oils.

METHODOLOGY

EXPERIMENTAL DESIGN FOR ENGINE OIL FORMULATION

To obtain the experimental engine oil formulation, a fractional factorial design was initially used to preliminarily evaluate the contributions of the proposed parameters and their appropriate ranges, with a reduced number of formulations. Subsequently, the response surface methodology was applied to obtain suitable mathematical models for the assessed responses and integrated optimization of the evaluated responses.

In the experimental design, 5 parameters listed in Table 1 were evaluated, with 2 levels and 2 central points repeated for each level of the categorical variable (Viscosity Index Modifier – VIM and additive package addition order).

Table 1. Parameters and levels used in experimental design

Parameter	Lower Level (Coding: -1)	Upper Level (Coding: +1)
Base Stock Ratio [Light Neutral/(Light Neutral+PAO4)]	0.25	0.75
VIM Content, % w/w	0.1	2
Additive Package Content, % w/w	7	10
Temperature, ºC	80	120
Additive Addition Order	PM: Additive Package-VIM	MP: VIM-Additive Package

In this context, for the 2^{5-1} fractional factorial design, 20 formulations were prepared, evaluating 2 characteristics based on the SAE J300 standard related to the SAE 0W 30 grade specification, that is, a low-temperature viscosity (CCS at -35 ºC) and a high-temperature viscosity (kinematic viscosity at 100 ºC) and two others related to the oil's corrosive potential (Acidity Index and Basicity Index). The viscosity grade was chosen for comparison with the commercial SAE 0W 30 API SN Plus engine oil used in GDI engine tests.

A protocol to perform Response Surface Methodology (RSM) [8] was subsequently applied to obtain suitable mathematical models for explaining the phenomena and to find the best region for optimizing responses. Given that values higher than the maximum level and lower than the minimum level would generate inconsistencies, the RSM used star points $\alpha = 0.5$. All points were evaluated under both conditions of the categorical variable, with a repetition for the central points.

To prepare the mixtures randomly according to the proposed plan, the following parameters were set:

- Mass: 200 grams
- Mechanical stirrer rotation rate: 270 revolutions per minute
- Ester content: 8% by mass
- Homogenization time at the evaluated temperature level: 1 hour for the first three components (PM: Base Stock + Ester + Additive package and MP: Base Stock + Ester + Viscosity Index Improver) and 1 hour after adding the remaining component (PM: Viscosity Index Modifier and MP: Additive package).

Base stocks levels evaluated were derived from technical report nº 2/2016 - Overview of Base Stocks in Brazil (published by National Agency of Petroleum, Natural Gas and Biofuels – Brazil), that is, demands related to Group I base stocks, such as Light Neutral, both occurring in 2000 and forecasted for 2030 (approximately 75 % and 25 %), whose trend is the loss of demand for more noble base stocks, such as polyalphaolefins. The levels used for the package content were based on the manufacturer's recommendation and the Viscosity Index Modifier (VIM) content in a typical formulation for engine oil [9]. In a preliminary evaluation, it was found that a homogenization time of 1 hour at 80 ºC was enough for solubilizing the VI Modifier (considering all the components of the formulation), and thus, it was decided to use this temperature as the lower level, limiting the upper level to 120 ºC for safety reasons.

GDI ENGINE TESTS

Tests were conducted on a turbocharged GDI engine, using hydrated ethanol (E100) and gasoline C (E27) as fuels, according to current Brazilian regulations. The same test conditions were maintained for the different fuels, such as the total engine operation time and cyclic load profile. The commercial engine oil used - SAE 0W 30 API SN Plus, was entirely replaced for each test.

LABORATORY ENGINE OIL AGING

A similar apparatus to that proposed by [5], with a cooling bath and a 60 cm condensation column with an internal spiral, was used to age the commercial and experimental engine oils in the laboratory, simulating product degradation conditions, as shown in Figure 2.

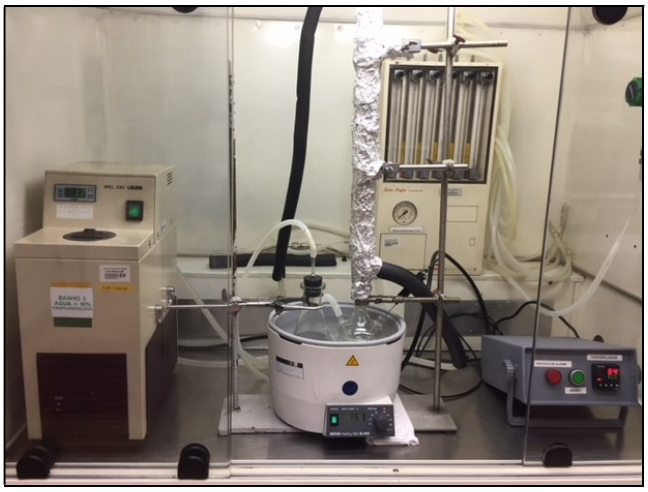

Figure 2. Apparatus for laboratory engine oil aging

For this purpose, the following conditions were used:

- Total mass: 350 grams - the required amount for testing.
- Flow rate of synthetic air: 10 L/h [5].
- Temperature of the liquid mass: 95 ºC - simulation of the oil temperature in the crankcase of a turbocharged GDI engine [3].
- Cooling bath temperature: 18 ºC - the temperature required for vapor condensation up to the maximum height of 30 cm of the column (50 % of the total height).
- Contamination by ethanol and its combustion residues: 9 % w/w - an estimate based on the maximum contamination by fuel (gasoline RON = 93) observed in engine oil of a turbocharged GDI engine with the oil temperature maintained at 95ºC [3]. Ethanol contamination includes doping with acetic acid at 0.028 % w/w content, calculated based on the relative increase in AN observed in the commercial engine oil used in GDI engine test when fueled with hydrated ethanol, specified by Brazilian Regulation.
- Aging time: 8 hours - simulation of the maximum daily usage time of a vehicle for professional purposes, according to Law No. 13103, of March 2, 2015 [10].

TYPICAL ENGINE OIL TESTS

The engine oils evaluation adhered to the ASTM test methodologies outlined below, carried out according to the objective of the evaluation to which the products were subjected:

- Kinematic Viscosity (KV) – ASTM D445:2017
- Specific Gravity – ASTM D4052:2018
- Cold Cranking Simulator (CCS) – ASTM D5293:2017
- Acid Number (AN) – ASTM D664:2017
- Base Number (BN) – ASTM D2896 A:2015
- Copper Strip Corrosion – ASTM D130:2018
- Water Content – ASTM D6304:2016

ELECTROCHEMICAL IMPEDANCE SPECTROSCOPY (EIS) TESTS

For EIS tests, a copper wire was soldered to both metallic materials (copper strip and ferrous material) to ensure electrical contact (Figure 3). Copper test samples were then embedded in epoxy resin, and the ferrous material samples (connecting rod bearing) were coated with paint on the front side. The areas of the metallic samples were 1 cm² for copper strip and 7 cm² for ferrous material. The evaluation of the metallic behavior in engine oil samples was conducted by monitoring EIS over immersion time.

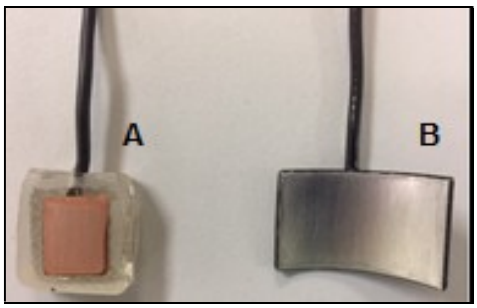

Figure 3. Copper (A) and ferrous material (B) used for EIS tests

The electrochemical impedance spectroscopy was performed using an AUTOLAB PGSTAT302N potentiostat-galvanostat, between frequencies of 100 kHz and 10 mHz. The volume of oil used was 125 mL, in an electrochemical cell containing a platinum counter electrode, a silver/silver chloride reference electrode, and working electrodes made of copper (prepared according to ASTM D130 methodology) or ferrous material (connecting rod bearing from a GDI engine).

Metallic samples were initially polished with 360 grit sandpaper, rinsed with ethyl alcohol, and dried with a cold air jet, remaining immersed in the test products for a period of 28 days at a temperature of (22.3 ± 1.8) ºC. The potential values were continuously monitored with the aid of the potentiostat and the saturated Ag/AgCl reference electrode throughout the entire immersion period of the metallic samples (working electrodes). The impedance diagrams were recorded using the reference electrode (saturated Ag/AgCl) and the counter-electrode (platinum) at times t = 0 (immediately after immersion), t = 14 days, and t = 28 days, and at amplitudes of 50 mV and 100 mV. Engine oil (EO) samples used are listed as follows:

- EO-1: Fresh commercial engine oil
- EO-2: Commercial engine oil after E100 engine tests
- EO-3: Commercial engine oil after E27 engine tests
- EO-4: Fresh experimental engine oil
- EO-5: Experimental engine oil partially laboratory aged (with heating only, no ethanol and its combustion residues added)
- EO-6: Experimental engine oil fully laboratory aged
- EO-7: Commercial engine oil fully laboratory aged

RESULTS

Initially, a fractional factorial 2^{5-1} design was conducted to perform an initial screening of the parameters with a reduced number of formulations. Compositional parameters and operational conditions were evaluated to obtain a typical engine oil, whose viscosity characteristics are related to the SAE J300 standard, and the acid and base numbers infer conditions for corrosion protection [11].

According to the viscosities and corrosion protection results for fractional factorial design, absolute influences (mean of absolute variation of each response due to the change from the lower to the higher level of the factor – Table 1) and contributions based on the sum of squares (deviation of the values of each treatment around the overall mean of the data) of the factors and double interactions were obtained from Design Expert® software – version 11 and presented in Figure 4. The following codes were adopted to the factors: A – Components Addition Order; B – Base Stock Ratio; C – MIV Content, % w/w; D – Additive Package Content, % w/w; E – Temperature, ºC. AB, AC, AD, AE, BC, BD, BE, CD, CE, and DE codes are regarded to the factor's double interactions.

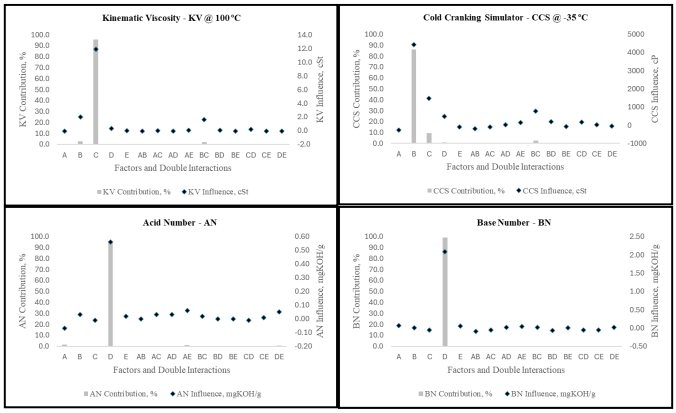

Figure 4. Influences and contributions - factors and double interactions

It is observed that the kinematic viscosity at 100ºC is primarily influenced by viscosity index modifier (VIM) content, which is a polymer that, at elevated temperatures, alters its conformation to subtly modify this property. For this reason, higher viscosity index values are obtained when greater amounts of VIM are used [1]. Base stock ratio [Light Neutral/(Light Neutral+PAO4)], followed by the interaction of this factor with the MIV content, complete, in this order, the major contributions to the kinematic viscosity result. According to the influence calculation, VIM content varying from 0.1% to 2.0% increases the kinematic viscosity result at 100 ºC, on average, by 11.88 cSt in this formulation. Since the lowest level (0.1%) is insufficient to meet the minimum specification limit and the highest level (2.0%) exceeds the range, an intermediate concentration of VIM is necessary to meet the SAE J300 specification for SAE 0W 30 grade.

For Cold Cranking Simulator (CCS) dynamic viscosity, performed at low temperature, the most relevant factor is the type of base stock that composes the formulation, with VIM being the second largest contributor, followed by the interaction between both. Therefore, in formulation design, it must be considered that, to achieve the desired viscosities, whether at high or low temperatures, not only the individual factors of the base oil type and viscosity index improver polymer contribute, but also the interactions between them. According to the influence calculation, varying base stock ratio from 0.25 to 0.75 increases the CCS result at -35 ºC, on average, by 4429 cP in this formulation, requiring an intermediate base stock ratio to meet the SAE J300 specification for SAE 0W 30 grade. The increase in light neutral content (inferred by the increase in the base stock ratio), which is a Group I paraffinic mineral product rich in linear hydrocarbon chains, corroborates the increase in low-temperature viscosity. However, due to the high cost of Group IV synthetic base stock (PAO 4), which mostly has branched chains, it is convenient to use Group I to reduce the cost of obtaining the engine oil formulation [1].

For acid and base numbers, the major contribution is due to the additive package used, as it provides constituents of various chemical species such as long-chain carboxylic acids, amines, and sulfonates, used for performing various functions, such as anticorrosive, antioxidant, dispersant, and detergent. However, it is observed that, in the case of the acidity index, the second largest contributor is the order of VIM and additive package addition. For base number, the additive package showed a 99 % contribution percentage, indicating that compounds contributing to this property, such as organic sulfonate, are little influenced by other factors. According to the influence calculation, varying the concentration of the additive package from 7% to 10% increases the AN and BN, respectively, by 0.56 mg KOH/g and 2.08 mg KOH/g in this formulation, on average. These values indicate that for a 3% increase in the concentration of the additive package, there is an increase in basicity relative to acidity of approximately 4 times, which is beneficial for the final formulation concerning protection against corrosion by the neutralization mechanism of acidic components generated in the combustion process.

Table 2 summarizes data from the analysis of variance table obtained for the optimized models of the fractional factorial design 2^{5-1}, with interactions of up to 2 factors.

Table 2. p-value results for 2 factors interaction in 2^{5-1} factorial design

Response	Model	Curvature	Lack of Fit	R^2
KV @ 100 ºC	< 0.0001	< 0.0001	0.6113	1.0000
CCS @ -35 ºC	< 0.0001	< 0.0001	0.0271	0.9991
AN	< 0.0001	0.0112	0.2881	0.9920
BN	< 0.0001	0.8310	0.2297	0.9987

The obtained p-value results, i.e., the probability of significance, considering a 95 % confidence level (or a 5% significance level), indicate that models have statistical significance and represent the phenomena for the factors and ranges considered. However, the values obtained for viscosities and acid number curvatures also show they have significance (p-value < 0.05), and thus, the adopted design is not satisfactory to represent ranges of the studied factors, which was not observed for base number. Lack of fit, i.e., the significance of the fit performed by considering only the terms with up to 2 interactions, CCS viscosity at -35 ºC showed statistical significance (p-value < 0.05), indicating that model should include a greater number of terms to explain the phenomenon. Since models obtained in the fractional factorial design for viscosities and acid number do not provide adequate models, the RSM was used to perform an integrated optimization [8].

To revisit the points already studied in the fractional factorial design and evaluate internal points within the studied ranges, a value $\alpha = 0.5$ was used in the response surface methodology (RSM). This value was utilized so that all points were equally distributed within the study ranges to define the best surface model, with a greater number of levels compared to the factorial design. Table 3 presents all the results obtained for the MSR planning, encompassing all factorial, central, and axial points.

Table 3. Factors and Responses

Formula	FACTORS					RESPONSES			
	Base Stock Ratio	VIM Content, %w/w	Additive Package Content, % w/w	Temperature, °C	Components Addition Order (PM: Additive Package - VIM; MP: VIM - Additive Package	KV @ 100 °C, cSt	CCS @ -35 °C, cP	AN, mgKOH/g	BN, mgKOH/g
1	0.25	0.1	7.0	80	PM	4.682	2116	1.90	5.28
2	0.75	0.1	7.0	80	PM	5.123	6502	1.63	5.26
3	0.25	2.0	7.0	80	PM	16.02	2978	1.55	5.21
4	0.75	2.0	7.0	80	PM	20.15	7985	1.52	5.37
5	0.25	0.1	10.0	80	PM	4.878	2483	2.17	7.53
6	0.75	0.1	10.0	80	PM	5.377	6489	2.03	7.70
7	0.25	2.0	10.0	80	PM	16.52	3174	2.03	7.61
8	0.75	2.0	10.0	80	PM	20.84	9873	2.12	7.56
9	0.25	0.1	7.0	120	PM	4.797	2162	1.50	5.17
10	0.75	0.1	7.0	120	PM	5.177	5919	1.64	5.40
11	0.25	2.0	7.0	120	PM	16.08	2830	1.44	5.30
12	0.75	2.0	7.0	120	PM	19.95	8641	1.52	5.34
13	0.25	0.1	10.0	120	PM	4.843	2361	2.06	7.58
14	0.75	0.1	10.0	120	PM	5.311	6655	2.18	7.64
15	0.25	2.0	10.0	120	PM	16.50	3330	2.10	7.48
16	0.75	2.0	10.0	120	PM	20.70	8957	2.32	7.61
17	0.38	1.0	7.5	100	PM	9.323	3299	1.75	6.32
18	0.63	1.0	7.5	100	PM	10.13	5504	1.88	6.44
19	0.50	0.6	7.5	100	PM	6.934	3851	1.93	6.44
20	0.50	1.5	7.5	100	PM	13.57	4691	1.85	6.47
21	0.50	1.0	7.8	100	PM	9.663	4055	1.75	5.82
22	0.50	1.0	9.2	100	PM	9.693	4274	1.97	7.22
23	0.50	1.0	8.5	90	PM	9.682	4337	1.86	6.42
24	0.50	1.0	8.5	110	PM	9.563	4129	1.88	6.30
25	0.50	1.0	8.5	100	PM	9.728	4134	1.87	6.43
26	0.50	1.0	8.5	100	PM	9.701	4150	1.91	6.51
27	0.25	0.1	7.0	80	MP	4.689	2117	1.40	5.30
28	0.75	0.1	7.0	80	MP	5.058	6544	1.61	5.23
29	0.25	2.0	7.0	80	MP	16.15	3004	1.60	5.03
30	0.75	2.0	7.0	80	MP	19.99	8040	1.45	5.30
31	0.25	0.1	10.0	80	MP	4.840	2493	2.14	7.60
32	0.75	0.1	10.0	80	MP	5.317	6508	2.02	7.58
33	0.25	2.0	10.0	80	MP	16.50	3166	1.98	7.63
34	0.75	2.0	10.0	80	MP	20.74	9911	2.39	7.65
35	0.25	0.1	7.0	120	MP	4.640	2170	1.55	5.22
36	0.75	0.1	7.0	120	MP	5.133	5860	1.44	5.42
37	0.25	2.0	7.0	120	MP	16.11	2830	1.44	5.30
38	0.75	2.0	7.0	120	MP	19.26	8103	1.54	5.24
39	0.25	0.1	10.0	120	MP	4.843	2396	2.15	7.96
40	0.75	0.1	10.0	120	MP	5.336	6720	2.14	7.57
41	0.25	2.0	10.0	120	MP	16.54	3279	2.14	7.70
42	0.75	2.0	10.0	120	MP	20.40	8996	2.20	7.53
43	0.38	1.0	7.5	100	MP	9.323	3306	1.91	6.31
44	0.63	1.0	7.5	100	MP	10.12	5495	1.82	6.43
45	0.50	0.6	7.5	100	MP	7.006	3876	1.84	6.38
46	0.50	1.5	7.5	100	MP	13.60	4497	2.03	6.54
47	0.50	1.0	7.8	100	MP	9.683	4250	1.70	5.79
48	0.50	1.0	9.2	100	MP	9.795	4290	1.98	6.89
49	0.50	1.0	8.5	90	MP	9.719	4333	1.91	6.41
50	0.50	1.0	8.5	110	MP	9.624	4158	1.89	6.47
51	0.50	1.0	8.5	100	MP	9.585	4183	1.88	6.45
52	0.50	1.0	8.5	100	MP	9.675	4123	1.93	6.37

Model types obtained by RSM design, as well as the responses changes to fit the data to a normal distribution, i.e., "Box-Cox" change, are presented in Table 4. According to p-values obtained, all had statistical significance and non-significant lack of fit, meaning that exclusion of terms with significance probabilities greater than 5 % did not harm the model fit.

Table 4. RSM: Model types and their fitting characteristics

Response	Box-Cox Change	Model Type	Lack of Fit	R^2
KV @ 100 ºC	Natural logarithm	Reduced quadratic	0.2691	0.9998
CCS @ -35 ºC	Inverse square root	Reduced 2-factor interaction	0.0644	0.9963
AN	-	2-Factor interaction	0.1164	0.9146
BN	-	Linear	0.2869	0.9909

With mathematical models ready, optimization was carried out to obtain a formulation with a maximized base stock ratio, fixing the VIM percentages at the central point (1.0 % w/w) and the additive package as recommended by the manufacturer (8.6 % w/w). The temperature was set at the lower value for safety reasons, and the order of addition of the MIV components and the additive package was not fixed, allowing for either of the two cases (MP or PM). Regarding the responses, the sole

objective of the optimization was to fix the kinematic viscosity at the central point of the specified range for SAE 0W 30 grade (10.9 cSt). For these inputs, the optimization performed by the Design Expert® software - version 11 resulted in a value of 0.67 for the base stock ratio and considered the PM order for the addition of MIV and the additive package. The predicted results for the optimized formulation, obtained by the model, resulted in percentage errors of less than 5 % compared to laboratory analyses. The optimized formulation, coded as "EO-4" whose results are presented in Table 5, followed to electrochemical tests along with commercial engine oil SAE 0W 30 API SN Plus.

Table 5. Optimized Formulation Characteristics

	Parameters	Optimized Values (Model Predicted Responses)	Laboratory (ASTM) Responses Results	% Absolute deviation (Laboratory Results x Model Prediction)
Factors	Base Stock Ratio	0.67		
	VIM Content, % w/w	1.0		
	Additive Package Content, % w/w	8.6		
	Temperature, ºC	80		
	Additives Addition Order	PM		
Responses	KV @ 100 ºC, cSt	10.90	10.47	4.0
	CCS @-35 ºC, cP	6200	6454	4.0
	AN, mgKOH/g	1.89	1.97	4.1
	BN, mgKOH/g	6.51	6.57	1.0

Results of typical tests for engine oils evaluation are presented in Table 6, all of which were conducted only before the immersion of the corresponding test specimens, to assess characteristics regarded to samples corrosiveness.

Table 6. Typical tests for engine oils evaluation

Parameters	Samples						
	EO-1	EO-2	EO-3	EO-4	EO-5	EO-6	EO-7
Specific Gravity (20/4) ºC	0.8409	0.8437	0.8475	0.8643	0.8643	0.8640	0.8397
KV 100ºC, cSt	10.14	9.440	8.265	10.47	10.73	10.45	8.589
AN, mgKOH/g	1.85	2.40	2.81	1.71	1.67	5.70	5.78
BN, mgKOH/g	6.37	3.19	4.64	5.86	5.85	0.40	1.65
Water Content, mg/kg	1232	574	563	942	730	1496	2222
Copper Corrosion 3h, 100 ºC	1A	2D	2A	1A	1B	1B	2C

Upon evaluating the parameters, a considerable reduction in the base number and an increase in the acid number were observed in the samples derived from tests on the GDI engine (EO-2 and EO-3), compared to the raw sample (EO-1). This phenomenon indicates the generation of undesirable carboxylic acids during the combustion process [11]. Acids generation impacted the products corrosiveness to copper, resulting in high values on the ASTM D130 methodology scale. The viscosity reduction in

EO-2 and EO-3 compared to EO-1 reveals contamination by fuel [12]. Thus, it is inferred that commercial SAE 0W 30 API SN Plus, derived from GDI engine test with E27 gasoline (EO-3), has higher contamination by fuel components than the product derived from the test with E100 (EO-2). Conversely, the result of copper corrosiveness at an elevated temperature in EO-2 indicates ethanol generated components that provided a greater corrosive effect on engine oil. The water content in Sample 1 was higher than in EO-2 and EO-3; however, no negative influence on corrosiveness at 100 ºC was observed for that oil. For experimental oil, except for water content, no significant differences were observed in fresh oil samples (EO-4) and after aging with heating at 95 ºC (EO-5). However, for the samples aged in the laboratory and contaminated with ethanol and acetic acid, both for the experimental oil (EO-6) and commercial SAE 0W 30 API SN Plus (EO-7), higher water contents were observed compared to the original oils, due to alcohol [13] and acid [14] hygroscopicity. It is inferred that low water contents in samples derived from GDI engine (EO-2 and EO-3) may be related to temperatures close to 550 ºC on engine piston [15]. EO-6 (experimental oil aged with ethanol and acetic acid), although it presented high acidity values and a decrease in basicity compared to EO-4 (fresh experimental oil), did not indicate significant variations in density, viscosity, and copper corrosiveness at 100 ºC, unlike EO-7, which, in addition to presenting increased acidity and reduced basicity compared to the original oil (EO-1), showed high corrosiveness at high temperature and reduced viscosity. An ambiguous and contradictory result was obtained for a consolidated test typically used in the evaluation of lubricating oil quality, which can lead to erroneous interpretations, as EO-6, having high acidity and low basicity (alkaline reserve), should present high copper corrosiveness at 100 ºC [6].

Since the dipolar nature of lubricants allows the evaluation of their properties through electrochemical impedance analysis, the following analysis can be shown

The evaluation of lubricating oils by electrochemical impedance spectroscopy can be spatially performed according to the frequency of the potential amplitude being supplied to the medium. The high-frequency region, i.e., above 10 Hz (log f = 1), is related to phenomena occurring in the liquid bulk, representing conduction and dielectric relaxation processes in a non-aqueous colloidal system [7].

In bulk, various lubricant components can be found, such as free dipoles from additives, molecules corresponding to the base oil, and large clusters of additive inverse micelles and contaminants, such as particulate matter and water. Impedance diagrams are directly related to contaminants and additives contents, as well as size and shape of clusters. For frequencies above 1000 Hz, purely capacitive effects are approximately constant in all cases for the evaluated times, as there are no significant changes in phase angles (close to -90°) and impedance magnitudes. Therefore, for the evaluated conditions and materials, it was not possible to correlate time-dependent physicochemical changes with impedance data at frequencies above 1000 Hz. However, low capacitance observed indicates electric current transfer will occur through the electrophoretic mobility of additive molecules and clusters dispersed in base stock.

In frequency range from 1000 Hz to 10 Hz, discrete distinctions show a transition between resistive and capacitive effects, with a single event observed in all cases. Thus, the equivalent circuit corresponding to this region consists of a capacitor and resistor in parallel, as shown in Figure 5.

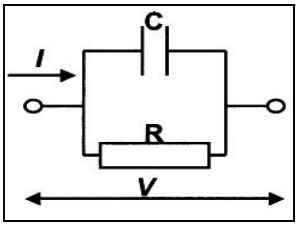

Figure 5. Equivalent circuit for bulk region, where C = capacitance, R = resistor, V = potential, I = electric current [6]

Mid-frequency range, between 10 Hz and 0,1 Hz (1 > log f > -1) [7], translates impedance characteristics related to charge accumulation due to the adsorption of active substances on the metal surface, such as anticorrosive, anti-wear, and detergent additives. In this region, characteristics of electric double layer, formed when charged species adhere to the electrode surface, are detected.

Inductive arcs were observed at 14 days of each metallic sample immersion in each EO, returning to capacitive arcs at 28 days, which were confirmed by positive phase angles. Adsorbed chemical substances organization on the metal surface occurs over time, governed by specific kinetics [16]. These substances may originate from the liquid bulk or from the oxidation of the electrode itself, originating from randomly distributed active sites on the surface, generating heterogeneous morphological changes. Surface changes related to the relaxation of adsorbates and roughness due to oxidation contribute to inductive arcs at frequencies in mHz magnitude order. Following this, inductive arcs appear when engine oil additives are adsorbed on metal surfaces [6].

Since the additive molecules organization on metal surface does not occur immediately, impedance readings immediately after test specimens' immersion in engine oils showed random shapes and characteristics, which did not result in concrete conclusions related to the effects occurring in the mid-frequency region. Therefore, only 14 and 28 immersion days were used to compare the effects of oils and their contaminants on ferrous material and copper foil surfaces, mainly at low frequencies, as the phenomena occurring in this region are directly impacted by molecular organization on the surface. Inductive arcs present at 14 days and converted to capacitive arcs at 28 days may indicate high electrode activity at the initial time, which is mitigated and thus converted to a capacitive condition due

to the growth of the layer of substances or films adsorbed at the interface [17].

The nanometer-scale distance between electrode charges and polar molecules acting on the surface generates the electric double layer effect, where a potential drop due to charge gap provides a capacitive effect. Since these capacitors are not ideal, given the electrodes porosity, surface heterogeneity, and consequent non-uniform current distribution, it is considered, for equivalent circuit purposes, that a double-layer pseudocapacitor (DLC) is in parallel with a charge transfer resistance (CTR). In all evaluated cases, phase angles in the mid-frequency region between 0° and 90° can be observed, indicative of capacitors in parallel with resistors, as well as, in some tests, the occurrence of inductive arcs observed at lower frequencies.

When evaluating impedance magnitudes (|Z|) at an intermediate frequency of mid-frequency range (1 Hz), and considering the influence of the test specimen area as presented in Table 7, it was observed that at 14 immersion days, fresh commercial engine oil (EO-1) showed a higher value for copper and ferrous material compared to fresh experimental oil (EO-4). This indicates a greater efficacy of inhibitory compounds present on the metallic surfaces. For commercial oil samples from GDI engine tests, |Z| value observed for copper after 14 days was approximately the same in both conditions (engines fueled with E100 and E27) and, for ferrous material, higher in case of E27, indicating greater surface protection in this condition.

Table 7. Impedance magnitudes at 1 Hz after 14 immersion days

Sample	|Z| (MΩ)	
	Copper	Ferrous Material
EO-1	1344	4607
EO-2	600	552
EO-3	491	1741
EO-4	382	1167
EO-5	382	1294
EO-6	243	1903
EO-7	836	3861

Regarding experimental oil and its aging only at 95 °C without contamination, after 14 days and 1 Hz, the |Z| values remained approximately constant for copper and ferrous material, demonstrating the low oxidative effect of this temperature on the oil during the aging time (8 hours). However, for aging simulations with ethanol and acetic acid contamination, copper |Z| values for both commercial and experimental oils were lower compared to fresh oils, as well as for ferrous material in commercial oil. It was not observed in ferrous material when immersed in experimental oil, as this value was higher for the same evaluation time. This indicates that, compared to the commercial engine oil, the experimental oil was more effective in protecting against iron corrosion due to the adsorption of species that hinder electric current transfer on the surface.

In mid-frequency range, the equivalent circuit corresponding to the evaluation at 14 days, except for the immersion of the ferrous material electrode in experimental oil, is represented by Figure 5, which presents the double-layer pseudocapacitor (DLC) in parallel with the charge transfer resistance (CTR), an inductor (L), and a resistor (R) and this R is regarded to the electrode polarization resistance. For other cases, including the evaluation at 28 days, equivalent circuit has the format represented by Figure 6, i.e., adsorption is represented by a pseudocapacitor in series with the charge transfer resistance.

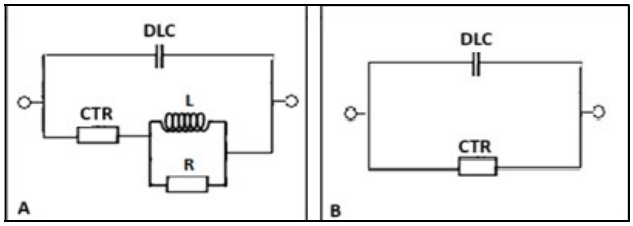

Figure 6: Equivalent circuit for mid-frequency at 14 immersion days (A) and 28 immersion days (B), where DLC = double-layer pseudocapacitor, CTR = charge transfer resistance, L = inductor, R = resistor [6]

Low frequence range, between 0,1 Hz and 0,01 Hz ($-1 > \log f > -2$), translates diffusion and charge transfer processes at electrode-oil interface. In all cases, predominantly resistive characteristics are observed, i.e., with phase angles close to zero, regardless of applied frequency, and therefore, no charge accumulation in the region between the metal and the adsorbed substance layer [7].

Point where $f \rightarrow 0$ corresponds to the metal polarization resistance, i.e., the measure of how much the integrity of this material can be preserved without electro-dissolution and consequent metal diffusion into liquid bulk, with this resistance being a direct process occurring at interface, evaluated in the mid-frequency region. Table 8 summarizes the results of the metallic potentials and polarization resistances (obtained at f = 0,01 Hz and already considering the area effect) after 28 days of immersion of the metals in the lubricating oils, as well as the variation in the concentration of these metals in the liquid mass (Δ Copper and Δ Iron). Although the concentration variations were considered null in the samples from the engine tests, given the high concentrations in the initial samples, small variations, undetected by the ASTM D6595 methodology may have occurred.

Table 8. Metallic potentials, polarization resistances and variations in copper and iron contents after 28 immersion days

Sample	Copper			Ferrous Material		
	Open Circuit Potential, mV	Polarization Resistance, MΩ	Δ Cu, mg/kg	Open Circuit Potential, mV	Polarization Resistance, MΩ	Δ Fe, mg/kg
EO-1	-595	2777	1.3	-374	2424	0
EO-2	76	2607	0	-244	2577	0
EO-3	-35	1291	0	-329	2920	0
EO-4	-267	1087	2.9	-360	2248	0
EO-5	-339	1391	6.2	-354	2548	0
EO-6	-367	1742	25.3	-408	4183	0
EO-7	-432	807	6.1	-371	6168	0

The highest relative increase in was observed in copper specimen immersed in EO-6, given the high amplitude between the AN and BN (Table 6). This occurred due to a possible weak action of the detergent additive (organic sulfonate) and/or copper corrosion inhibitor (nitrogenous aromatic compound), leading to metal attack and initial dissolution, generating copper in liquid mass. The highest polarization resistance in this case, compared to the other experimental oil samples, indicates that a film formed by the copper present in the liquid mass acts as a protective layer on the surface, under low turbulence conditions. According to the copper potential observed in samples from the GDI engine test, there is a low tendency for corrosion at the evaluated temperature, which can be corroborated by the lower water content in these samples. Regarding ferrous material, no significant differences were observed among the samples in potential and variations in iron content in the lubricating mass, according to the ASTM D6595 methodology. The polarization resistances to ferrous material are higher compared to those obtained for copper in most cases.

Simulating conditions of a GDI engine stopped at room temperature after 28 days of its last operation fueled with E100 or E27, generates a greater condition of corrosion protection for the engine internals made of copper and iron, because of corrosion inhibiting substances and/or protective film formation, phenomena observed by the respective impedance modules resulting from the lowest evaluated frequency (10 mHz). However, high temperature and turbulence generated during engine operation can lead to removal of this protection, with the consequent corrosion process progression.

CONCLUSIONS

According to the results obtained for engine oils formulations, RSM presented adequate models. Optimization carried out to obtain the semi-synthetic oil used in the electrochemical tests resulted in a base stock ratio of 0.671, i.e., a higher content of Group I (Light Neutral) compared to Group IV (PAO 4). Optimized formulation responses obtained by RSM model, compared to ASTM methodologies, were consistent, showing mathematical models were satisfactory (deviations of less than 5 %). Thus, this method can be promising in predicting the best compositions and parameter responses in engine oils developments, whether for new formulations, process corrections, component replacement, and composition and/or operational optimizations, aiming at both cost reduction and performance improvement.

Regarding the effect of ethanol on commercial SAE 0W 30 engine oil, after an operation cycle in a GDI engine fueled with hydrated ethanol and gasoline containing anhydrous ethanol at 27 % v/v, fuel contamination in second case was more pronounced, given the greater drop of viscosity compared to fresh oil. Despite the higher acidity obtained in engine oil from E27 test, product from engine fueled with E100 caused greater corrosivity to copper at high temperature. In ferrous material, no evidence was observed to prove corrosive attack on this material under the evaluated conditions.

Physicochemical results showed that, in the simulation of an engine stopped for 28 days after the operation cycle at room temperature and without turbulence, the copper blade oxidizes as much in contact with used oils as with fresh oils, to a lesser extent in the latter case. This fact shows that, even at low temperature, copper is attacked, either by oxygen diffusion from the air or by the action of substances present in the liquid mass. This oxidation, however, favors the mitigation of the engine oil's corrosivity to the engine internals made of copper, because of corrosion inhibiting substances and/or protective film formation, phenomena observed by the behavior of the respective impedance modules resulting from the lowest evaluated frequency (0,01 Hz). However, high temperatures and turbulence during GDI engine operation can lead to the removal of this protection, with consequent corrosive process progression. Artificial aging performed by simulating the feeding of the engine with hydrated ethanol led to high AN values and reduced BN compared to the reference sample (from the engine test fueled with E100), which would represent the use of the lubricant beyond the recommended, i.e., when such indices equalize.

Temperature for simulating the crankcase condition (95°C) did not cause significant change in these values and other characteristics, as evaluated with the experimental oil.

EIS technique proved to be very sensitive and promising in evaluating engine lubricating oils, both for fresh and used products. These results were consistent with physicochemical tests regarding copper, as the material adhered to the surface was beneficial in increasing the metal polarization resistance under engine stopped at room temperature. This could not be confirmed for ferrous material, as such a surface alteration was not observed in all evaluated engine oils. In summary, there is a tendency for increased engine oil corrosivity in GDI engines with higher ethanol content in fuel, especially for copper components, under engine operating conditions.

REFERENCES

[1] RIZVI, Syed Q. A. *A Comprehensive Review of Lubricant Chemistry, Technology, Selection and Design*. West Conshohocken, PA: ASTM International, 2006. 635 p.

[2] DAEMME, Luiz Carlos et al. Emissão de Material Particulado em Veículos Flex Fuel de Injeção Direta de Combustível. In: *PRêMIO AEA DE MEIO AMBIENTE*, 10., 2016, São Paulo. Anais.... São Paulo: Associação Brasileira de Engenharia Automotiva, 2016. p. 1 - 20.

[3] HU, Tingjun et al. Impact of Fuel Injection on Dilution of Engine Crankcase Oil for Turbocharged Gasoline Direct-Inject. *SAE International Journal Of Engines*, [s.l.], v. 8, n. 3, p.1107-1116, 14 abr. 2015. SAE International. http://dx.doi.org/10.4271/2015-01-0967.

[4] GANI, Rafiqul; NG, Ka M.. *Product Design: From Molecules to Formulations to Devices*. In: INTERNATIONAL CONFERENCE ON FOUNDATIONS OF COMPUTER-AIDED PROCESS DESIGN, 8., 2014, Washington. Proceedings. Washington: Elsevier B.v., 2014. p. 108 - 123.

[5] BESSER, Charlotte et al. Investigation of long-term engine oil performance using lab-based artificial ageing illustrated by the impact of ethanol as fuel component. *Tribology International*, [s.l.], v. 46, n. 1, p.174-182, fev. 2012. Elsevier BV. http://dx.doi.org/10.1016/j.triboint.2011.06.026.

[6] LVOVICH, Vadim F. *Impedance Spectroscopy: Applications to Electrochemical and Dielectric Phenomena*. New Jersey: John Wiley & Sons, 2012. 353 p.

[7] LVOVICH, Vadim F.; SMIECHOWSKI, Matthew F.. Impedance characterization of industrial lubricants. *Electrochimica Acta,* [s.l.], v. 51, n. 8-9, p.1487-1496, jan. 2006. Elsevier BV. http://dx.doi.org/10.1016/j.electacta.2005.02.135.

[8] CURIC, Anamarija et al. Formulation optimization of itraconazole loaded PEGylated liposomes for parenteral administration by. *International Journal Of Pharmaceutics*, [s.l.], v. 448, n. 1, p.189-197, maio 2013. Elsevier BV. http://dx.doi.org/10.1016/j.ijpharm.2013.03.029.

[9] SCHILOWITZ, ALAN M.; BAILLARGEON, DAVID J.; HAQUE, TABASSUMUL. *Lubricating oil compositions with engine wear protection*. US nº WO 2016109376 A1, 30 dez. 2014, 07 jul. 2016.

[10] PRESIDÊNCIA DA REPÚBLICA DO BRASIL. *Lei nº 13103, de 02 de março de 2015*. Brasília, DF: Casa Civil, Subchefia Para Assuntos Jurídicos.

[11] SOLEIMANI, Mostafa. et al. Engine oil acidity detection using solid state ion selective electrodes. *Tribology International*, [s.l.], v. 65, p.48-56, set. 2013. Elsevier BV. http://dx.doi.org/10.1016/j.triboint.2013.02.030.

[12] KHUONG, L. S. et al. A review on the effect of bioethanol dilution on the properties and performance of automotive lubricants in gasoline engines. *RSC Advances*, [s.l.], v. 6, n. 71, p.66847-66869, 2016. Royal Society of Chemistry (RSC). http://dx.doi.org/10.1039/c6ra10003a.

[13] FLORES, A.; CONDE, E.. Effect of the Hygroscopic Nature of Pure Ethanol in the Accuracy of Preparation of Simulator Solutions. *Volpe National Transportation Systems Center*. Cambridge, MA, p. 1-1. 30 jun. 2004. Disponível em: <https://rosap.ntl.bts.gov/view/dot/9419/dot_9419_DS1.pdf?>.

[14] MCMURRY, P.H.; SEINFIELD, J.H.. Organics Alter Hygroscopic Behavior of Atmospheric Particles. *Journal Of Geophysical Research*, S/i, v. 100, n. 9, p.755-770, 20 set. 1995.

[15] WANG, Xinyan et al. Numerical Study of the Effect of Piston Shapes and Fuel Injection Strategies on In-Cylinder Conditions in a PFI/GDI Gasoline Engine. *SAE International Journal Of Engines*, [s.l.], v. 7, n. 4, p.1888-1899, 13 out. 2014. SAE International. http://dx.doi.org/10.4271/2014-01-2670.

[16] CÓRDOBA-TORRES, P.; KEDDAM, M.; NOGUEIRA, R.P. On the intrinsic electrochemical nature of the inductance in EIS—A Monte Carlo simulation of the two-consecutive steps mechanism: The rough 3D case and the surface relaxation effect. *Electrochimica Acta*, [s.l.], v. 54, n. 27, p.6779-6787, nov. 2009. Elsevier BV. http://dx.doi.org/10.1016/j.electacta.2009.06.084.

[17] CHEN, Kongfa; AI, Na; JIANG, San Ping. Origin of low frequency inductive impedance loops of O 2 reduction reaction of solid oxide fuel cells. *Solid State Ionics*, [s.l.], v. 291, p.33-41, ago. 2016. Elsevier BV. http://dx.doi.org/10.1016/j.ssi.2016.04.021

CONTACT INFORMATION

CHARLESLB@PETROBRAS.COM.BR